REPORT DOCUMENTATION PAGE

Form Approved
OMB No. 0704-0188

1. REPORT DATE *(DD-MM-YYYY)*
08/10/2007

2. REPORT TYPE
Final Performance Report

3. DATES COVERED *(From - To)*
February 1, 2004 to June 30, 2007

4. TITLE AND SUBTITLE
Improved Control Authority in Flexible Structures Using Stiffness Variation

5a. CONTRACT NUMBER
AFOSR Contract # FA 9550-04-1-0069

5b. GRANT NUMBER

5c. PROGRAM ELEMENT NUMBER

5d. PROJECT NUMBER

5e. TASK NUMBER

5f. WORK UNIT NUMBER

6. AUTHOR(S)
Mukherjee, Ranjan
Shaw, Steven, W.

7. PERFORMING ORGANIZATION NAME(S) AND ADDRESS(ES)
Michigan State University
301 Administration Building
East Lansing, MI 48824-1226

8. PERFORMING ORGANIZATION REPORT NUMBER

9. SPONSORING/MONITORING AGENCY NAME(S) AND ADDRESS(ES)
Air Force Office of Scientific Research
875 North Randolph Street, Suite 325
Arlington, VA 22203
Dr Victor Giurgiutu/NA

10. SPONSOR/MONITOR'S ACRONYM(S)
AFOSR

11. SPONSOR/MONITOR'S REPORT NUMBER(S)

AFRL-SR-AR-TR-07-0460

12. DISTRIBUTION/AVAILABILITY STATEMENT
Approved for public release.
distribution [illegible]

13. SUPPLEMENTARY NOTES

14. ABSTRACT
This research investigated control authority enhancement in structural systems through methodical stiffness variation. Our early work focused on stiffness variation in a cantilever beam under the application of a buckling-type end force and control designs based on switching of the end force. Towards the end of the project, our modeling, control, and experimental methods were extended to truss-like structures. An important extension of the work was tuning of beam-type MEMS resonators through stiffness variation generated by follower and axial end forces. In addition to structural control using end forces, switching strategies were developed for piezoelectric transducers to enhance controllability and observability of flexible structures. By switching the transducers between actuator and sensor modes, we demonstrated the possibility of reducing control system hardware. A significant portion of our effort focused on modal energy redistribution through stiffness variation with the objective of simplifying control design. The energy flow between modes in different stiffness states was quantified and validated through preliminary experiments.

15. SUBJECT TERMS
Flexible structures, stiffness variation, switched stiffness, structural control, modal energy redistribution, modal disparity, piezoelectric transducers, cable actuators, follower force, axial force, MEMS resonator

16. SECURITY CLASSIFICATION OF: a. REPORT	b. ABSTRACT	c. THIS PAGE	17. LIMITATION OF ABSTRACT	18. NUMBER OF PAGES	19a. NAME OF RESPONSIBLE PERSON
U	U	U	UU	11	Ranjan Mukherjee
					19b. TELEPHONE NUMBER *(Include area code)* 517-355-1834

IMPROVED CONTROL AUTHORITY IN FLEXIBLE STRUCTURES USING STIFFNESS VARIATION

AFOSR Contract #FA 9550-04-1-0069

PI: Ranjan Mukherjee
Department of Mechanical Engineering
Michigan State University
East Lansing, MI 48824-1226
Ph: (517) 355-1834; Fax: (517) 353-1750
Email: mukherji@egr.msu.edu

Co-PI: Steven W. Shaw
Department of Mechanical Engineering
Michigan State University
East Lansing, MI 48824-1226
Ph: (517) 432-3920; Fax: (517) 353-1750
Email: shawsw@egr.msu.edu

Summary:

The main goal of this research was to improve control authority in structural systems through methodical stiffness variation. Our early work focused on variation in stiffness of a cantilever beam under the application of a buckling-type end force and control designs based on switching of the end force. A cable was used to apply the end force on the beam, and towards the end of the project our modeling, control, and experimental methods were successfully extended to truss-like structures. An important extension of the work was tuning of beam-type MEMS resonators through stiffness variation brought about by application of follower and axial end forces. In addition to the work on control using end forces, switching strategies were developed for piezoelectric transducers to enhance controllability and observability of flexible structures. By switching the transducers between actuator and sensor modes, we demonstrated the possibility of reducing control system hardware, both theoretically and experimentally. A significant portion of our work investigated modal energy redistribution in flexible structures due to stiffness variation with the underlying objective of simplifying control design. In the sequel we provide some of the important results obtained in course of our research.

(A) Vibration Suppression in a Cantilever Beam using a Buckling-Type End Force:

Consider the cantilever beam with end force P as shown in Fig.A1. Assuming Euler-Bernoulli beam theory and small deflections, it can be shown that P is a buckling-type end force (with an instability limit four times higher than the usual buckling load) and the equation of motion of the beam in Fig.A1 can be written as follows

$$\dot{x}_1 = x_2, \qquad \dot{x}_2 = -Kx_1 - Dx_2 + Cx_1 u \tag{1}$$

Figure A1. A flexible cantilever beam with an end force

where, x_1 and x_2 are vectors of modal displacements and velocities, $u = P$ is the control input, D is the matrix of modal damping, and K and C are given in Nudehi, et al. (2006).

The task of vibration suppression is to design the control input u that remains below the buckling load and guarantees asymptotic stability of the equilibrium $(x_1, x_2) = (0, 0)$. This goal can be achieved with the control system block diagram in Fig.A2, shown below (Nudehi, et al., 2006).

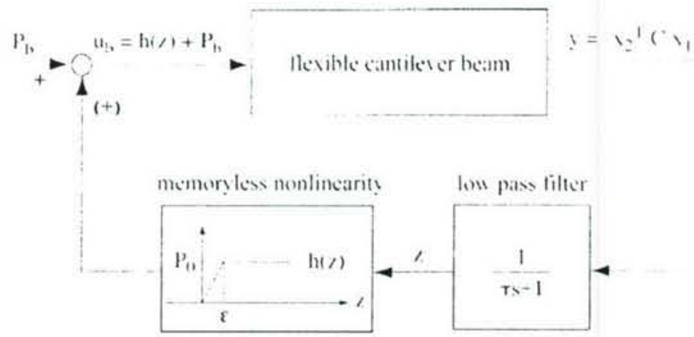

Figure A2. Control design based on bias tension and output filtering

The low-pass filter discards high frequency components and eliminates the requirement of high actuator bandwidth without adversely affecting the stability of the system. The memoryless nonlinearity is introduced to represent the fact that the cable can only provide a compressive force on the beam, and is defined as

$$h(z) = \begin{cases} P_0 & for \quad z \geq \varepsilon \\ P_0 z / \varepsilon & for \quad 0 \leq z < \varepsilon \\ 0 & for \quad z < 0 \end{cases} \tag{2}$$

In Fig.A2, P_b denotes the bias tension in the cable. There are two main advantages of applying a bias tension in the cable and these are discussed in Nudehi, et al. (2006).

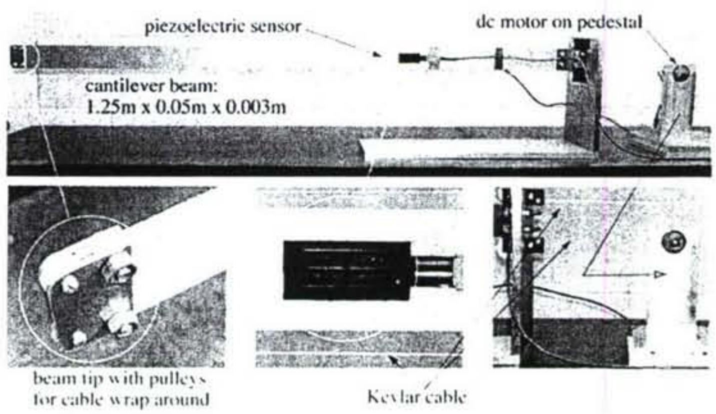

Figure A3. Experimental setup

We conducted experiments with the cantilever beam shown in Fig.A3. In our experiments, we considered the first two modes of the beam. The results in Fig.A4 were obtained with different combinations of bias tension, P_b, and the maximum control force, P_0. For all three experiments, the value of τ was kept fixed at 0.2 secs. The results demonstrate the efficacy of our control design.

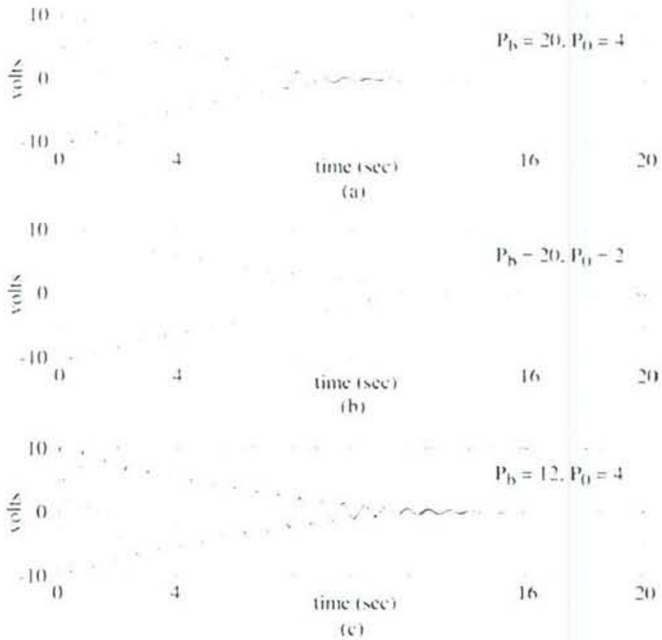

Figure A4. Vibration suppression in a cantilever beam using a buckling-type end force.

(B) MEMS Resonator Tuning using Follower and Axial End Forces:

The goal of this effort was to achieve significant improvements in the available tuning range of MEMS resonators by using a novel configuration of comb drives to provide end loads on a vibrating micro-beam. The basic mechanics can be demonstrated using a simple micro-cantilever beam model which has both a follower force F and an axial end load P applied to its free end, as shown in dimensionless form in Fig.B1. Under the usual assumptions of the elementary theory of bending, one can solve for the natural frequencies of the beam for different values of the follower force, σ, and axial force, η. Of particular interest here is the variation in the fundamental natural frequency of the beam with variation in the magnitude of the axial force when the follower force is zero (Fig.B2a), and variation in the frequencies of the beam with variation in the magnitude of the follower force when the axial force is zero (Fig.B2b). This can be exploited in the design of MEMS resonators whose first natural frequency can be tuned up or down through the application of axial and follower end forces (Singh, et al., 2005).

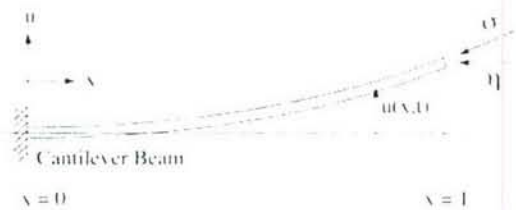

Figure B1. A MEMS cantilever beam with axial and follower end forces

Figure B2. Variation in natural frequency with change in (a) axial force (b) follower force

A schematic of the resonator, shown in Fig.B3, has a set of anterior combs for the application of the end force (axial or follower) and an additional set of lateral combs for actuation and sensing. The actuator combs were used to provide sinusoidal excitation for resonance whereas the sensor combs were used for real-time measurement of the beam deflection. Although the beam motions will remain small, all curved elements were designed by taking the local radius of curvature of the beam deflection (corresponding to the first mode shape) into consideration. This ensured that the gaps between the fixed and moving elements remained constant and prevented potential malfunctioning due to varying gap size or mechanical contact.

For the MEMS resonator in Fig.B3, (details in Singh et al., 2005) the first natural frequency was approximately 7.5 KHz. To realize a pure follower force, voltages V_A and V_B, at the fixed elements A and B, were found to be

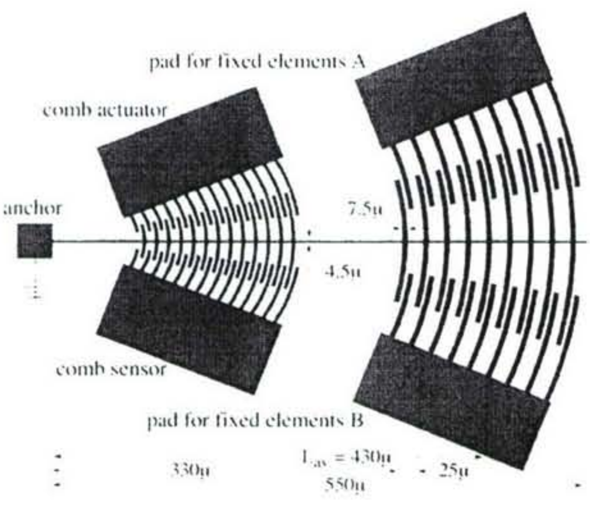

Figure B3. MEMS resonator designed at MSU

$$V_A = V_0\sqrt{\frac{(\alpha-\beta)\sin[(\alpha+\beta+\theta)/2]}{(\alpha-\beta+\theta)\sin[(\alpha+\beta)/2]}} \quad (3)$$

and

$$V_B = V_0\sqrt{\frac{(\alpha-\beta)\sin[(\alpha+\beta-\theta)/2]}{(\alpha-\beta-\theta)\sin[(\alpha+\beta)/2]}} . \quad (4)$$

For a purely axial force, the voltages are

$$V_A = V_0\sqrt{\frac{(\alpha-\beta)\sin[(\alpha+\beta-\theta)/2]}{(\alpha-\beta+\theta)\sin[(\alpha+\beta)/2]}} \quad (5)$$

and

$$V_B = V_0\sqrt{\frac{(\alpha-\beta)\sin[(\alpha+\beta+\theta)/2]}{(\alpha-\beta-\theta)\sin[(\alpha+\beta)/2]}} \quad (6)$$

where, α, β, and θ are defined in Singh, et al., (2005). For $V_0 = 70$ volts, it can be shown that the first natural frequency can be tuned down by 425 Hz and tuned up by 1.1 KHz. Thus, bi-directional frequency tuning of 1.5 KHz, that is, 20%, can be achieved.

(C) Enhancing Controllability and Observability by Switching Piezo Transducers:

The problem of vibration suppression in flexible structures, such as space structures, typically requires large number of sensors and actuators for sensing and control of multi-modal vibration. The sensors and actuators commonly used in the flexible structures are piezoelectric transducers (PZT) and the hardware associated with these transducers add significantly to the cost and weight of the system. For example, the power amplifiers used for piezoelectric actuators are much more expensive than the actuators themselves and contribute to the bulk of the weight of the complete control system. A large number of sensors, on the other hand, require a large number of analog-to-digital conversion channels in the data acquisition hardware. To reduce cost, weight, and volume of hardware required for the control system, switching strategies have been developed for sensing and control. Based on the theorem stated below, we have proposed to continuously switch the roles of the PZT actuators and sensors so as to obtain a system with an effective number of actuators and an effective number of sensors that is equal to the total number of PZT elements on the flexible structure. This approach can potentially reduce the number of actuators and sensors by 50%.

The basic theory is as follows. Consider the linear time-varying system that switches between the following two descriptions:

$$\begin{aligned} \Sigma_1: \quad \dot{x} = Ax + B_1 u \quad y_1 = C_1 x \\ \Sigma_2: \quad \dot{x} = Ax + B_2 u \quad y_2 = C_2 x \end{aligned} \tag{7}$$

If $x = (x_1^T x_2^T x_3^T)^T$, where $x_1 \varepsilon R^p$ is controllable and observable (CO) for both Σ_1 and Σ_2, $x_2 \varepsilon R^q$, $q \neq 0$, is controllable but unobservable ($C\bar{O}$) for Σ_1 and uncontrollable but observable ($\bar{C}O$) for Σ_2, and $x_3 \varepsilon R^r$, $r \neq 0$, is $\bar{C}O$ for Σ_1 and $C\bar{O}$ for Σ_2, then:

(1) $\{A, B_1\}$, $\{A, B_2\}$ are not completely controllable but $\{A, [B_1, B_2]\}$ is controllable,

(2) $\{A, C_1\}$, $\{A, C_2\}$ are not completely observable but $\{A, [C_1^T, C_2^T]^T\}$ is observable

(3) All the states of the switched system can be steered to the origin in finite time using estimated states if and only if the number of switchings is two or more.

A proof of this result can be found in the paper by Nudehi, et al. (2004).

A cantilever beam can be described using Eq.(7) when the piezo-transducers guarantee controllability when all of them are actuators and they guarantee observability when all of them are sensors. Thus, simple Luenberger observers can be designed for the sub-systems which results in the two closed-loop systems

$$\dot{X} = A_{c1} X, \quad \dot{X} = A_{c2} X, \quad A_{ci} = \begin{bmatrix} A & -B_i K_i \\ L_i C_i & A - B_i K_i - L_i C_i \end{bmatrix}$$

where X is comprised of the states of the beam, x, and their estimates, and K and L are controller and observer gains (Nudehi, et al., 2004). Given a total time duration of t_f secs and m switchings, the problem reduces to finding the switching times $t_i, i = 1, 2, ..., m$, that satisfy $0 \leq t_1 \leq t_2 \leq ... \leq t_m \leq t_f$ and minimizes the cost function $J = \int_0^{t_f} (X^T Q X) dt$ where Q is a constant positive definite matrix.

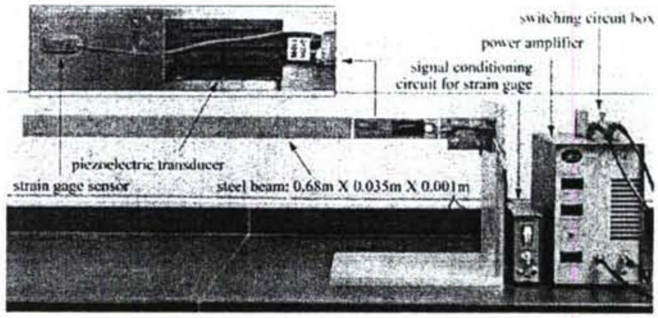

Figure C1. Experimental hardware used with switching piezoelectric transducers

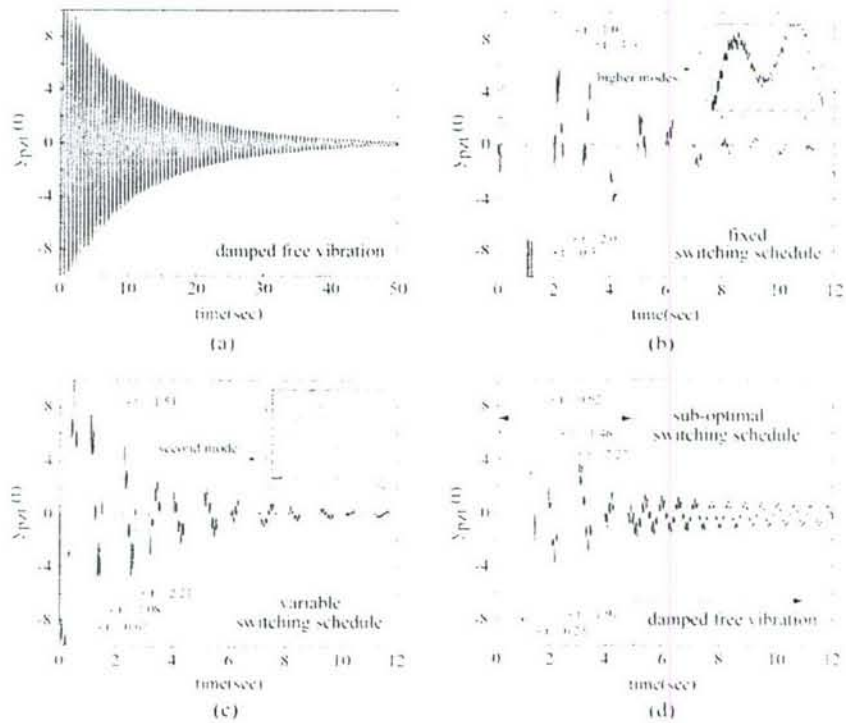

Figure C2. Experimental results of cantilever beam using a single piezo transducer switched between actuator and sensor modes: (a) uncontrolled system, (b) controlled system with fixed switching, (c) variable switching, and (d) optimal switching.

This problem is solved using Lyapunov equations; the details of the optimization procedure can be found in Nudehi, et al. (2004). Here we show experimental results for $m = 10$ and $t_f = 5.0$ secs. The optimal switching instants were found to be

$$t_1, t_2, ..., t_{10} = 0.25, 0.92, 1.46, 1.91, 2.27, 2.96, 3.47, 3.94, 4.23, 4.74 \tag{8}$$

The experimental hardware is shown in Fig.C1 and the experimental results in Fig.C2. The experimental results show that switching piezos between actuator and sensor modes can excite higher-order unmodeled dynamics, but this problem can be remedied by using a variable-time switching schedule (Nudehi, et al., 2004). In summary, this strategy shows great promise in providing effective control of structural vibrations using significantly less hardware than standard approaches.

(D) Vibration Suppression in Flexible Structures Exploiting Modal Disparity:

The idea behind the control strategy using modal disparity is to generate energy redistribution from a set of modes (not to be directly controlled) to a set of controlled modes through changes in the stiffness of the system. In this manner one can cause energy to flow from non-controlled to controlled modes in a systematic manner, thereby providing control access to many modes of vibration while controlling only a small number of modes. However, the change in stiffness must be done thoughtfully, since if a non-controlled mode in one stiffness state is nearly identical to a non-controlled mode in the other stiffness state, then modal energy will drain very slowly from these modes. For many structures, this is indeed the case, especially for higher modes, and hence a measure of modal disparity is needed to assess the effectiveness of this vibration control strategy. Two specific functions have been developed (we discuss one of them here) to measure modal disparity and we have investigated structures where stiffness variation is generated by switching levels of tension in cables connected to specific locations in the structure. To achieve maximum redistribution of energy, the positioning of the cables can be selected by means of a problem in topology optimization seeking to maximize modal disparity.

The theory is summarized as follows. A modal analysis of a structure in two stiffness states leads to two eigenvalue problems, such as the following:

Stiffness State 1: $$(\mathbf{K}^0 - \lambda\mathbf{M})\mathbf{u} = \mathbf{0} \tag{9}$$

Stiffness State 2: $$(\mathbf{K}^0 + \Delta\mathbf{K} - \mu\mathbf{M})\mathbf{v} = \mathbf{0} \tag{10}$$

where eigenpairs $(\mathbf{u}^{(i)}, \lambda_i)$ are associated with the free vibration of the baseline structure while eigenpairs $(\mathbf{v}^{(i)}, \mu_i)$ are associated with the free vibration of the structure augmented by the device used to change the structure's stiffness, e.g., cables, active joints or links. The contribution of these devices is represented by the added stiffness term $\Delta\mathbf{K}$.

In general, the products $\mathbf{u}^{(i)T}\mathbf{M}\mathbf{v}^{(j)}$ are *not* zero. Specifically, the projection of mode $u^{(i)}$ onto the space spanned by the $v^{(j)}$s is given by $\mathbf{u}^{(j)} = \sum_{i=1}^{N} a_{ij}\mathbf{v}^{(i)}$, where, from orthogonality properties of mode shapes, $a_{ij} = \mathbf{v}^{(i)T}\mathbf{M}\mathbf{u}^{(j)}$. The magnitudes of these projections provide a measure of modal disparity between the system it its two states. More formally, let I_C be the index set of controlled modes and I_{NC} be the index set of the not-controlled modes in the structure. When a change in stiffness is introduced, the system is switched from state 1 with modes u to state 2 with modes v. The not-controlled modes $u^{(j)}$, $j \in I_{NC}$ have a projection on the space spanned by controlled modes $v^{(i)}$, $i \in I_C$. The magnitude of this projection is measured by $f_{12} = \sum_{j \in I_{NC}} \sum_{i = I_C} a_{ij}^2$. The situation is similar when going from stiffness state 2 to state 1, yielding $f_{21} = \sum_{j \in I_{NC}} \sum_{i = I_C} a_{ji}^2$. Since the goal is to maximize energy transfer from uncontrolled to controlled modes, our goal is to maximize $\Phi_1 = \frac{1}{2}(f_{12} + f_{21}) = \frac{1}{2}\sum_{j \in I_{NC}} \sum_{i = I_C} a_{ij}^2 + a_{ji}^2$.

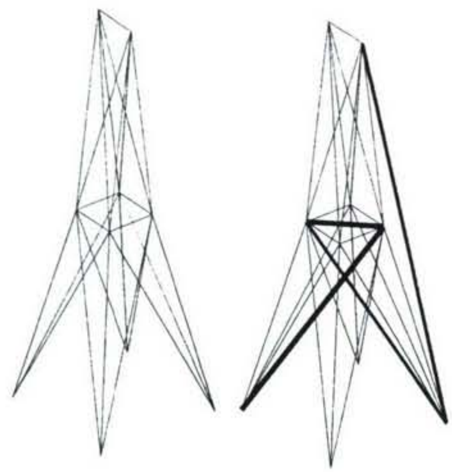

Figure D1. Structure and cable system and solution

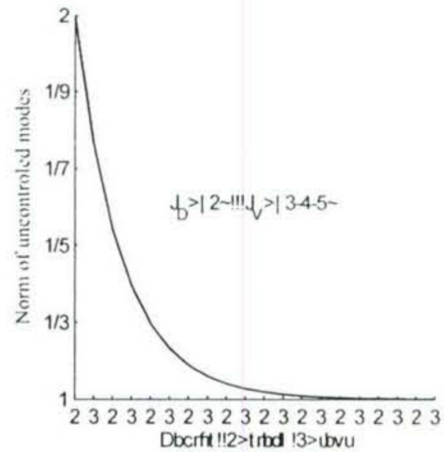

Figure D2. Decay of not-controlled modes

The example in Fig.D1 illustrates the optimization problem. The structure is tower-like and supported (pinned) at the base. The structure is 15.24 m (600 in) tall and 5.08 m (200 in) wide at the base and has 20 members. Details are given in Diaz and Mukherjee (2005). In this example we control mode 1, i.e. I_C={1}, and the not-controlled modes are I_U={2,3,4}. We seek solutions with 4 cables and apply a constant tension T= 2.22 kN (500 lb). A maximum static deflection of 2.5 mm (0.1 in) of any node in any direction is allowed under the cable action. The topology optimization results in a non-symmetric cable layout that maximizes modal disparity between the two states. During free vibration only one mode in each state is controlled, and after 20 on/off switches, the vibration energy in all modes, including those not directly controlled, is significantly reduced (see Fig.D2). Similar to the strategy described in part (C), this approach offers effective vibration control with significantly fewer actuators and sensors than standard approaches.

The concept of modal disparity and redistribution of energy due to change in stiffness was demonstrated through experiments (Issa, Mukherjee, Diaz, and Shaw). The experimental setup, shown in Fig.D3, is a beam clamped at both ends with a mid-span hinge that can be locked or set free by an electromagnetic brake. The stiffness of the beam is dependent on the state of an electromagnetic brake built in the hinge. Two cases are considered, the beam is in stiffness state α when the hinge is free and in stiffness state β when the hinge is locked. Transition from on state to another is assumed to occur over a brief interval of time and achieved by locking or releasing the hinge. Let $\left[t^{+}_{\alpha\beta}, t^{-}_{\alpha\beta}\right]$ and $\left[t^{+}_{\beta\alpha}, t^{-}_{\beta\alpha}\right]$ denote the transition periods from stiffness state α to β and from stiffness state β to α. Finite elements was used to model the beam in its both states. If Φ and Ψ are the beam's modal matrices in state α and β respectively and M its mass matrix, the modal amplitudes and velocities right before and right after the transition period are found to be related through the following equations:

$$
\begin{aligned}
\nu\left(t^{+}_{\alpha\beta}\right) &= \Psi^{T} M \Phi \, \mu\left(t^{-}_{\alpha\beta}\right) & \qquad \mu\left(t^{+}_{\beta\alpha}\right) &= \Phi^{T} M \Psi \, \nu\left(t^{-}_{\beta\alpha}\right) \\
\dot{\nu}\left(t^{+}_{\alpha\beta}\right) &= \Psi^{T} M \Phi \, \dot{\mu}\left(t^{-}_{\alpha\beta}\right) & \qquad \dot{\mu}\left(t^{+}_{\beta\alpha}\right) &= \Phi^{T} M \Psi \, \dot{\nu}\left(t^{-}_{\beta\alpha}\right).
\end{aligned}
\qquad (11)
$$

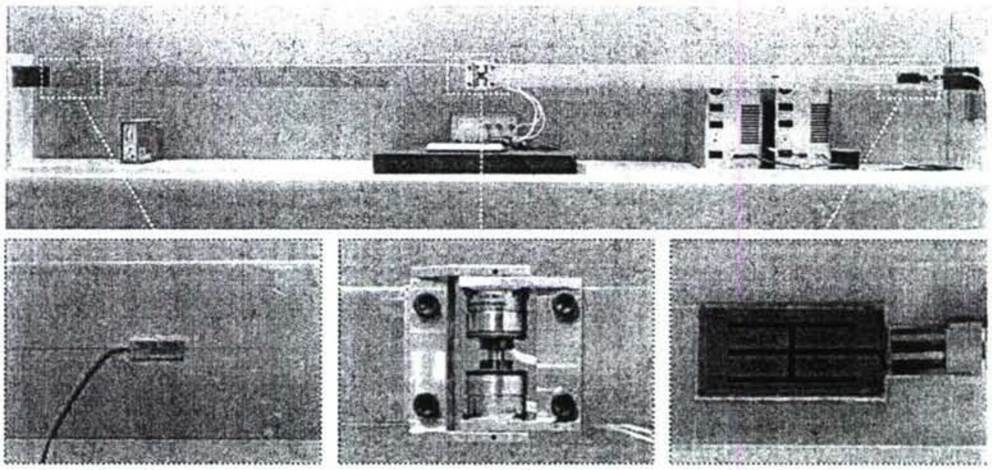

Figure D3. Clamped-clamped beam with mid-span hinge. The hinge is locked and set free by activating and de-activating an electromagnetic brake to change stiffness and demonstrate modal disparity

In the above equation, $\mu(t)$ and $\nu(t)$ are the vector of modal amplitudes in state α and β respectively, evaluated at time t. It is clear that $\Psi^{T} M\Phi$ define the mapping between modal coordinates during the transition from stiffness state α to stiffness state β, similarly its transpose $\Phi^{T} M\Psi$ defines the mapping between modal coordinates during the transition from stiffness state β to stiffness state α. These matrices define a measure of modal disparity between the two stiffness states of the beam.

The experimental procedures are described next. A pair of piezoelectric transducers was used for excitation and a piezoelectric strain sensor was used for sensing as shown in Fig.D3. The amount of modal energy redistributed between the modes in the two stiffness states matched the values calculated numerically using the mapping matrices in Eq.(11). One specific experimental result is shown in Fig.D4. In this case the beam was excited at its third mode of stiffness state α. It was switched to stiffness state β after termination of the excitation. Energy was transferred from the first mode in state α to the first and third mode of state β. No energy was transferred to the second mode, this is due to symmetry of the beam where the even-numbered modes are not affected by the state of the hinge thus energy in these modes will remain in them after changing the state of the beam.

Acknowledgements:

The PI would like to thank Professor Alejandro Diaz for collaborating on optimization problems for maximizing modal disparity in structures.

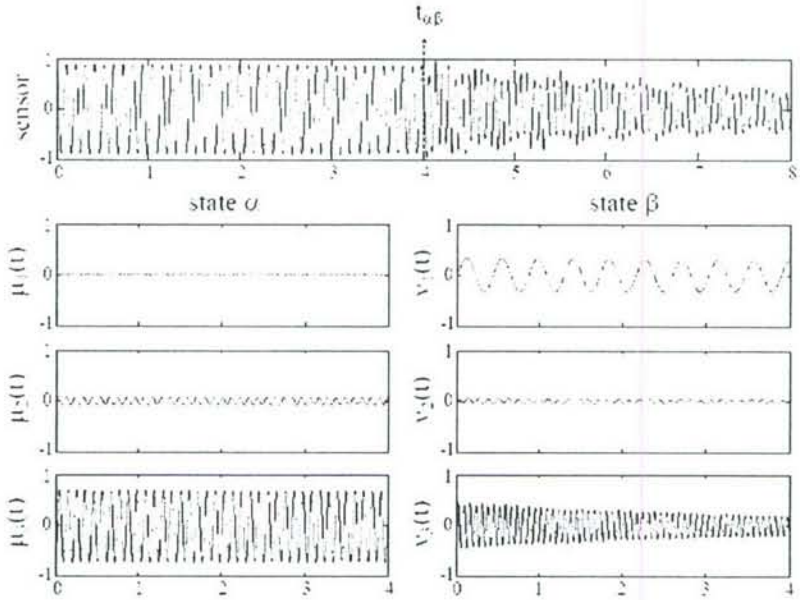

Figure D4. Demonstration of modal disparity in clamped-clamped beam.

References:

(1) Nudehi, S., and Mukherjee, R., 2004, "Enhancing Controllability/Observability in Under-Actuated/Under-Sensed Dynamical Systems through Switching: Application to Vibration Control", ASME Journal of Dynamic Systems, Measurement, and Control, Vol.126, pp.790-799.

(2) Singh, A., Mukherjee, R., Turner, K., and Shaw, S. W., "MEMS Implementation of Axial and Follower End Forces", Journal of Sound and Vibration, Vol.286, No.3, pp.637-644, 09/2005

(3) Diaz, A., and Mukherjee, R., "Modal Disparity Enhancement through Optimal Insertion of Non-Structural Masses", Structural and Multidisciplinary Optimization, Vol.31, No.1, pp.1-7, 01/2006

(4) Diaz, A., and Mukherjee, R., "A Topology Optimization Problem in Control of Structures using Modal Disparity", ASME Journal of Mechanical Design, 128, pp.536-541, 05/2006

(5) Nudehi, S., Mukherjee, R., and Shaw, S. W., "Active Vibration Control of a Flexible Beam using a Buckling-Type End Force", ASME Journal of Dynamic Systems, Measurement and Control, Vol.128, pp.278-286, 06/2006

(6) Issa, J., Mukherjee, R., Diaz, A., and Shaw, S. W., "Modal Disparity and its Experimental Verification", Journal of Sound and Vibration, (accepted for publication).

PhD Dissertation Research Supported by the Contract:

Hybrid Control of Flexible Structures, PhD Dissertation, Department of Mechanical Engineering, Michigan State University, December 2005